ORIGINAL ARTICLE

https://doi.org/10.21708/avb.2024.18.2.12019

Characterization of cobalt ferrite nanoparticle and evaluation its toxic effect in experimental mice

Caracterização de nanopartículas de ferrita de cobalto e avaliação de seu efeito tóxico em camundongos experimentais

Nasr Tarq[1], Huda Sadoon[2], Ahmed Alshammari[3]

ABSTRACT: This study investigated the characterization of cobalt ferrite nanoparticles (CoFe2O4) prepared by the pulsed laser deposition (PLD) method, using various techniques such as energy-dispersive X-ray spectroscopy (EDX), X-ray diffraction (XRD), scanning electron microscopy (SEM), Fourier transform infrared spectroscopy (FTIR), and in vitro drug release test (IVRT). It also evaluated the toxicity of these nanoparticles on liver, spleen, heart, and kidney tissues using a mouse model. $CoFe_2O_4$ nanoparticles were synthesized from an aqueous solution containing 1mg of $CoFe_2O_4$ powder dissolved in DMSO and RPMI serum-free media. XRD analysis revealed the characteristic peaks of the spinel lattice of cubic-shaped cobalt ferrite nanocrystals, with an average crystallite size of 12 nm calculated using Scherrer's formula. SEM and EDX were used to study the surface morphology and chemical compositions, respectively. The in vivo experiments determined the LD50 of $CoFe_2O_4$ to be 3000 mg/kg body weight. Administration of $CoFe_2O_4$ nanoparticles at a dosage of 75 mg/kg body weight for 14 days did not cause any changes to the histological structure of the tissues in the mouse model, indicating their potential biocompatibility.

KEYWORDS: nanoparticles; CoFe2O4; cytotoxicity; mouse model; histopathological.

RESUMO: Este estudo investigou a caracterização de nanopartículas de ferrita de cobalto (CoFe2O4) preparadas pelo método de deposição a laser pulsado (PLD), utilizando várias técnicas como espectroscopia de raios-X por dispersão de energia (EDX), difração de raios-X (XRD), microscopia eletrônica de varredura (SEM), espectroscopia infravermelha por transformada de Fourier (FTIR) e teste de liberação de medicamento in vitro (IVRT). Também avaliou a toxicidade dessas nanopartículas nos tecidos do fígado, baço, coração e rins usando um modelo de camundongo. As nanopartículas de CoFe2O4 foram sintetizadas a partir de uma solução aquosa contendo 1mg de pó de CoFe2O4 dissolvido em DMSO e mídia RPMI livre de soro. A análise de XRD revelou os picos característicos da estrutura de espinélio de nanocristais de ferrita de cobalto em forma de cubo, com um tamanho médio de cristalito de 12 nm calculado usando a fórmula de Scherrer. SEM e EDX foram utilizados para estudar a morfologia da superfície e as composições químicas, respectivamente. Os experimentos in vivo determinaram que a DL50 do CoFe2O4 é de 3000 mg/kg de peso corporal. A administração de nanopartículas de CoFe2O4 na dose de 75 mg/kg de peso corporal por 14 dias não causou alterações na estrutura histológica dos tecidos no modelo de camundongo, indicando sua potencial biocompatibilidade.

PALAVRAS-CHAVE: nanopartículas; CoFe2O4; citotoxicidade; camundongo modelo; histopatológico.

INTRODUCTION

The unique properties of nanoparticles encourage the belief that they can be applied in a wide range of fields, from medical applications to environmental sciences, this can lead to increasing the quality of life via early diagnosis and treatment of disease due to their multifunctional properties such as small size, superparamagnetism, and low toxicity (Sumaiah *et al.*,2019).

In addition, NPs can enhance the intracellular concentration of drug in the cells, while avoiding toxicity in normal cells,

College of Veterinary Medicine/University of Baghdad, Email: alnasr_tarq@yahoo.com
College of Veterinary Medicine/University of Baghdad
Iraqi center for cancer and medical genetic research ICCMGR, Collage of medicine/AL mustansyria university
*Corresponding author: (Nasr T.M)
Received: 06/19/2023. Accepted: 12/12/2023

and due to their antioxidant activities, some NPs act against the damaging effects for some drugs (Sood and Khudiar,2019).

Nanoparticles are divided into various types based on their chemical composition, including organic and inorganic nanoparticles, cobalt ferrite nanoparticles among organic metal oxide nanoparticles which are more stable than organic nanostructures, and inorganic structures that are arranged as three-dimensional structures with connected atoms. (Salas, *et al*., 2012).

Spinel ferrites have the formulae MFe_2O_4 with a face-centered cubic symmetry, where M is the metal donates. Spinel ferrites have eight tetrahedral sites and sixteen octahedral sites for M^{2}+ and Fe^{3}+ ions to occupy. All metallic cations occupy the tetrahedral position, while all Fe^{3}+ ions occupy the octahedral position. (Pacakova *et al.,* 2017).

As the particle size of magnetic material falls to nanoscale levels, one of the most striking size-dependent features of magnetic particles is a rise in ionic conductivity, anisotropy, and coercivity, among other things, in comparison to bulk material (Mukta *et al.,*2009). The term "ferrite" refers to a class of ferrimagnetic oxides that are composed of ferric oxides and metal oxides. In terms of their crystal structures, ferrites can be divided into 3 distinct categories: spinel ferrite, garnet ferrite, and hexagonal ferrite. Because of the diverse range of applications that spinel ferrites have, they are the subject of a significant amount of research. Spinel ferrites can accommodate cations with a variety of valences in their interstitial positions, which can result in a wide range of variations in their electrical and magnetic characteristics. (Nlebedimn *et al.,*2010).

The purpose of this work is to evaluate the structure and electrical properties of cobalt ferrite nanoparticles that have been produced using the PLD method. There are not many reports on the toxicity of Fe_3O_4, particularly under in vivo settings, and the conclusions have been contested. For instance, some research has revealed non-toxic effects under in vivo settings, while others have shown little toxicity at certain dosages. Other researchers have described minimal toxicity (Kim *et al.,* 2006). In vivo, studies have shown that some subjects experienced liver and kidney damage, as well as abnormalities in their gastrointestinal and neurological systems (Arora *et al.,* 2012; Amiri and Shokrollahi 2013). Because of this, this study was carried out to examine the characteristics and the toxicity of Cobalt/Ferrite nanoparticles on the tissues of the liver, kidney, heart, and spleen.

MATERIAL AND METHOD

Preparation of Cobalt ferrite nanoparticle stock

The source of Cobalt ferrite nanopowders was NANOCHEL company (India), $CoFe_2O_4$ size:12nm which was prepared by pressing 1g of cobalt ferrite powder into spherical pellets with a radius of 16mm and a height of 3mm using a hydraulic compressor under 10Tons of pressure. The pulse laser depositing method PLD was used to deposit $CoFe_2O_4$ directly onto the glass container in a single step. A 100µl DMSO(dimethyl sulfoxide) and 4900 µl Rosswell Park Memorial Institute (RPMI)-1640 , Medium serum-free media, and Minimum Essential Medium (MEM) media to obtain 5ml in clean sterilized glass, in which each ml contain 200 µg/ml of $CoFe_2O_4$ nanoparticles(Mohammad *et al.,* 2020), and the solution was mixed by using sonication and vortex, filtered by Millipore membrane filter 0.4µm that is positioned above the pellet within the vacuum chamber of the PLD device, which runs with a background pressure of 2.5 times* 10-2 mbar,900 V and 1cm distance at different energies for 200 pulses. The surface of the pellet was brought into sharp focus by directing the laser beam through a lens with a focal distance of 120 millimeters., as shown in figure (1,2). The structural characteristics of the $CoFe_2O_4$ samples were determined by a) X-ray diffraction (XRD) this technique is used to characterize the crystal structure of $CoFe_2O_4$ nanoparticles powder, this system supplied with Cu-kα radiation at a wavelength of (λ = 0.154060 nm) produced at 40 kV. The samples were scanned over a range of (5°-40°) at room temperature,b) energy-dispersive X-ray spectroscopy (EDX) to detect the elemental composition of $CoFe_2O_4$ nanoparticles, and c) Scanning electron microscope(SEM) to determine the particle's size and topography,e) Fourier transform infrared spectroscopy(FTIR) was utilized to identify molecular components, structures and to get chemical

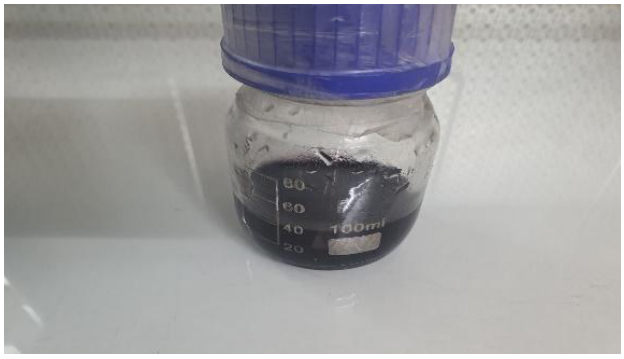

Figure 1. the stock solution of CoF_e2O_4

Figure 2. PLD device used in preparation of CoF_e2O_4

bonds of pure $CoFe_2O_4$ nanoparticles powder and in vitro drug release assay(IVRT) utilizing the dialysis bag method, the dialysis bags (MwCO8000-14000 Millipore, Boston, USA) were preloaded with 2 ml of $CoFe_2O_4$ dispersion and then left to soak in double-distilled water for 24 hours before being loaded with the dispersion. The laden bags were then placed in two conical flasks, with one bag being immersed in 100 ml of normal saline and the other bag being immersed in saline solution and HCL. The flasks were then placed in a water bath at 37 Cºwith a stirring rate of 100 revolutions per minute. When the sink conditions needed to be adjusted, the released medium was removed at intervals of 0.5, 1.0, 2.0, 3.0, 4.0, 5.0, 6.0, and 7.0 hours and replaced with same quantity of fresh media (Mora *et al.,*2009).

Determinatio the Acute Toxicity of Nanoparticles

The following steps were used to determine the LD50 of $CoFe_2O_4$NPs injected to mice by using single animals at each step, the dosage depending on whether the previously dosed animals lived or died. This method known referred to as the "up-and-down" approach, it was outlined by (Dixon, 1980):

- A series of concentrations of $CoFe_2O_4$NPs NPs was chosen with equal spacing (concentrations) between doses
- The dose was determined based on the total body weight of the mice, and it was injected intraperitoneally (IP).
- The starting dose was 2250mg/kg body weight from $CoFe_2O_4$ NPs24 hrs. after injection. If the animal remained alive the dose was increased but if it died reducing does.
- A sequence of trials was conducted using this rule: raise the dose in reaction to a negative response (i.e. Survived (O)), and lower the dose in response to a positive response (i.e. dead(X)).
- After being installed last dose, in which the loss occurred, following equation was applied: - **LD50= xf + kd.** As shown in Table 1.

The very important advantage of this method was required only eight or ten test animals as compared with the "classical" LD50 test (Bruce RD., 1985) that may be used (40 to 50) test animals. While the limitation of the Dixon approach is the long duration of the research. After the administration of the dose, each animal must be monitored for at least one week so that delayed death can be documented. (Wsfi *et al.,*2015).

Histopathology study

A total of 18 female swiss albino mice (6-8) weeks' age, (20-25g) weight housed and maintained in the Iraqi center for cancer and medical genetic research ICCMGR, under temperature-controlled circumstances (23. 5Cº). The animals were fed specific food pellets and were provided with clean water. Throughout the duration of the tests, each of the six animals was placed in a plastic cage with woody shaving bedding. The linens were changed regularly to maintain a sanitary environment.

The mice were separated into three groups of six mice each: As a negative control, Group one (G1) received an intraperitoneal injection, of sterile saline (10 mL/kg/7days). Group two (G2) received LD50% dose of $CoFe_2O_4$ NPs (3000 mg/kg) through intraperitoneal injection, while group three (G3) received $CoFe_2O_4$ NPs 1/40 of LD50% (75 mg/kg/ 7 days) via intraperitoneal injection (Eman *et al.,*2021). Post 14 days mice were sacrified, liver, kidney, heart and spleen tissues were harvested and washed with PBS then preserved in 10% formaldehyde solution for 24hrs. After removing excess fixative through washing, tissue samples were dehydrated in graded series of ethanol, clarified with xylene and embedded in histological paraffin. For histological investigation, sections were stained with hematoxylin and eosin (H&E) (Bancroft and Gamble 2008).

RESULTS AND DISCUSSION

A. Structural Properties

Structural and morphological studies of cobalt ferrite nanoparticles

The structural properties of the produced powder was investigated using X-ray diffraction (XRD) Figure (4-1): A close analysis of the XRD pattern indicates the presence of slightly broader peaks, indicative of the sample's small crystallite size. According to the Joint Committee on Powder Diffraction Standards (JCPDS) card number (22-1086) data all the characteristic peaks in the sample at angles 30°, 32.08°, 35. 5°, 18°, 28°, 36°, 43° ,57°,63° and 75° are indexed as the reflection planes of (220), (104), (311), (111), (222), (400), (422),(511),(400), and (622) respectively, which match the cubic spinel lattice of cobalt ferrite ($CoFe_2O_4$) nanocrystals as a single phase and no impurity peaks were observed in XRD (Sanpo and Wang,2013), the sharpest diffraction peaks

Tabl e 1 . shows Dixon values. Dixon (1980).

Initial dose mg/Kg .BW	Last dose mg/ Kg.BW	Difference between doses mg/Kg.BW	Number of animals	Outcome After 24 huOr	K*	LD50 mg/ Kg.BW
2250	2750	250	6	OOOXOXO	0.741	2935

O means survived animal, X means dead animal, Constant, f = latest given dose, K=Factor of change from the table, d= difference in dose levels.

reflect the nanocrystals' transparency (311) reflection represents the nanocrystalline nature of the spinel cobalt ferrite magnetic nanoparticles. The formula developed by Debye and Scherrer was used to determine the crystallite size, denoted by the letter D, of spinel cobalt ferrite magnetic nanoparticles (Amiri and Shokrollahi, 2013). Based on the XRD findings, the crystallite size is determined to be 12nanometers'as shown in Figure (3).

$$D = (k\lambda/\beta \cos \theta)$$

Where:
K is the Scherrer constant.
λ is wave length of the X-ray beam.
β is the Full width at half maximum (FWHM) of the peak.
θ is the Bragg angle.

The spinel ferrite is having the chemical formula MFe_2O_4 (where M- is an ion of a divalent metal such as Co, Ni, or Mn, etc.) and contain two main sites known as tetrahedral A sites and octahedral B sites. Spinel ferrites have the ability to accommodate cations with a variety of valences in their interstitial positions, which can result in a wide range of variations in their electrical and magnetic characteristics. Because of the combination of their electrical and magnetic properties, spinel ferrites are considered to be among the most important magnetic materials. Researchers from a variety of institutions have looked at the structural, electrical, and magnetic qualities of spinel ferrite in its bulk form (Nlebedimn *et al.,*2010). Energy-dispersive spectroscopy (EDS) studied $CoFe_2O_4$ nanoparticle surface topography and mineral composition (Prashant *et al.,*2018). Samples of cobalt ferrite are displayed in the EDS spectrum (figure) (4). Cobalt (Co), ferric (Fe), and oxygen (O) percentages of the sample are shown in Table 2 using EDS images.

Scanning electron micrographs (SEM) technique determine as shown in Figure (5)s the size, shape and surface morphology with direct visualization of cobalt ferrite nanoparticles. The morphology of the cobalt ferrite NPs in product a is comprised particle size, with narrow distribution in spherical/cubic form.. $CoFe_2O_4$ particles in SEM images appear to have some degree of aggregation is an indication of the nanocrystalline nature of the sample. (Mushtaq *et al.,*2016).

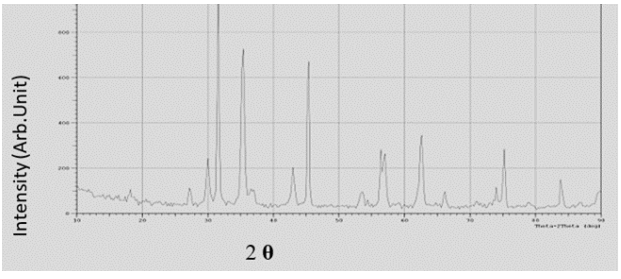

Figure 3. X-ray diffraction pattern for $CoFe_2O_4$ nanoparticles.

Because of its magnetic properties and the combination of particles bound together through weak surface interactions such as van der Waals forces, the images imply that there is a significant degree of agglomeration of ferrite particles. In addition to this, the nature of the surface topography is noted to be very porous in appearance (Ghazaleh *et al.,*2015). The transmission FTIR spectra of CoFe2O4 nanoparticle is an appropriate approach to determine the chemical and structural changes

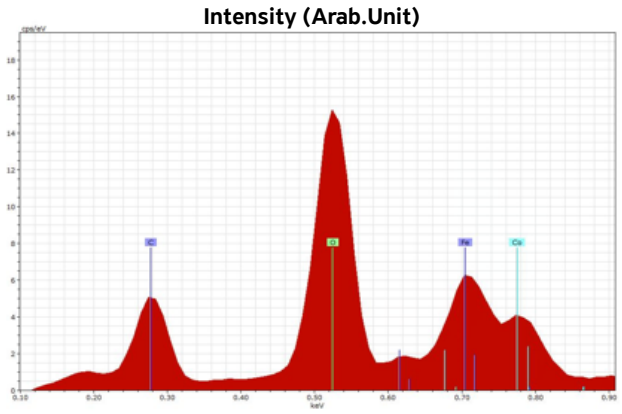

Figure 4. The EDS Spectrum of $CoFe_2O_4$nanoparticles.

Table 2. crystalline Size (C), percentage of cobalt (Co), ferric (Fe), and oxygen (O) of cobalt ferrite nanoparticles obtained from SEM and EDS.

No.	Parameter	Value
1	Crystaline size	12nm
2	Co	13.12%
3	Fe	35.78%
4	O	51.10%

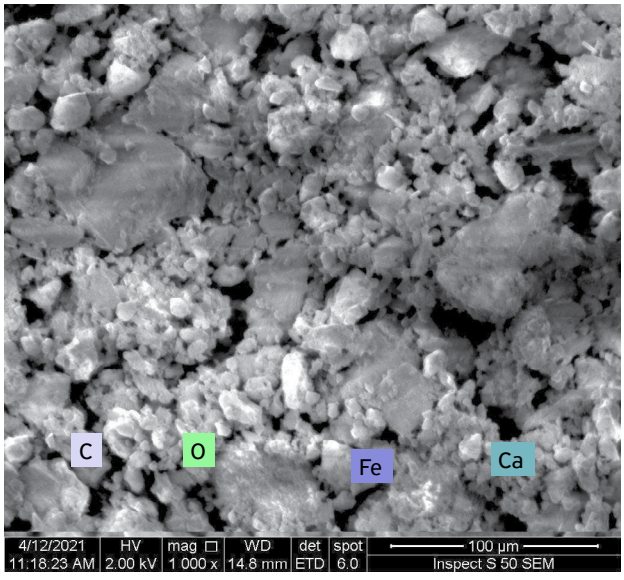

Figure 5. Scanning electron micrograph of $CoFe_2O_4$.

that are taking place in the materials as well as the places that the ions are occupying (Raut *et al.*, 2014).

Figure 6 displays the results of Fourier-transform infrared spectroscopy (FTIR) performed on the cobalt ferrite nanoparticles. The results show that the cobalt ferrite sample shows two vibration bands at wavelength range 597–615 (1) and at 412–400 (2) cm1, which correspond to the stretching vibration of the (M-O) bond in tetrahedral and octahedral sites, respectively. The results match two absorption bands at 435 and 592 cm-1 corresponding to Co-O and Fe-O bands, respectively (Hosseini et al.,2018). The other important peaks of the sample 842cm-1and ~ 1430cm-1corresponding to C-C and H-C-H bonds respectively. (Mahmoud et al.,2010).

A study by Kalam *et al.*, 2018 found that the high-frequency band in the range of 597–615 cm1 is caused by tetrahedral metal ion and oxygen complex vibrations, while the weak-frequency band in the range of 412–400 cm1 is caused by stretching of octahedral metal ion and oxygen complex. Results from the FTIR and XRD revealed that the samples contained a spinel structure of $CoFe_2O_4$.

To compare between the release of the sample in acidic and neutral environments,in vitro drug release assay(IVRT) was carried out using the dialysis bag method, the dialysis bags (MwCO8000-14000 Millipore, Boston, USA) were submerged in double-distilled water for twenty-four hours before being loaded with two milliliters of a CoFe2O4 dispersion. The laden bags were then placed in two conical flasks, with one bag being immersed in 100 ml of saline solution and the other bag being immersed in saline solution and HCL. The flasks were then placed in a water bath at 37 *C*°with a stirring rate of 100 revolutions per minute. When the sink conditions needed to be adjusted, the release media was removed at intervals of 0.5, 1.0, 2.0, 3.0, 4.0, 5.0, 6.0, and 7.0 hours and replaced with the equal volume of fresh medium as shown in figure (7) (Mora *et al.*,2009). It was observed that the drug release rate is higher at elevated temperature and acidic pH~5.5 as compared to normal temperature and pH~7. This provide suitable release of CoFe2O4NPs as anticancer drug (Chaitali *et al.*,2018) as shown in figure (8).

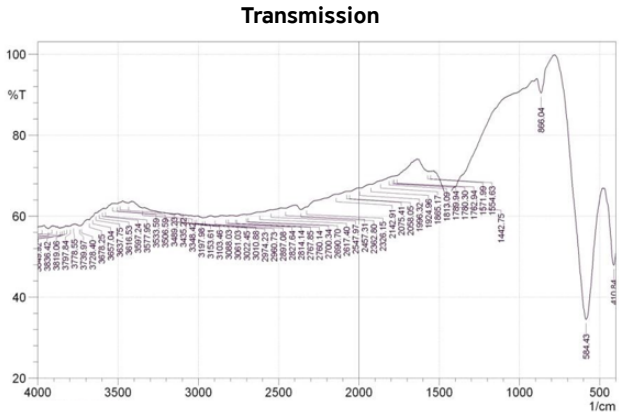

Wave number (Cm-1)

Figure 6. Fourier transforms infrared spectra of $CoFe_2O_4$

B- Evaluation the toxicity of Cobalt Ferrite in experimental mice.

Histological examination of liver sections taken from the negative control group (G1), which had 10 ml/kg intraperitoneally administered doses of sterile saline.; showed normal liver architecture with central vein, normal eosinophilic homogenous hepatocytes cytoplasm, mild nuclear enlargement, and mild sinusoidal dilatation. The heart shows normal cardiomyocytes with eosinophilic homogenous cytoplasm and regularly nucleoid vascular congestion (longitudinal &cross section). Histopathological section of mice kidney shows cortex and medulla with normal glomeruli and tubules apart from mild tubular dilatation. And finally, the section of the mice spleen shows normal white and red pulps with normal architecture apart from mild congestion. As shown in figure (9:G1).

In the group that was injected with $CoFe_2O_4$ nanoparticles (G2)1/40ofLD50% dose (75mg/kg b.w i.p) histopathological changes of mice liver shows normal central vein surrounded by few irregular sinusoids and normal looking hepatocytes, few others with enlarged nuclei and mild cytoplasmic degeneration. While a histopathological section of mice heart shows normal cardiomyocytes with eosinophilic cytoplasm with peripherally located nuclei. The kidney of the treated mice shows normal renal architecture including normal glomeruli and tubules, and regular Bowman's space with few tubular

Figure 7. In vitro drug release assay (IVRT) of $CoFe_2O_4$

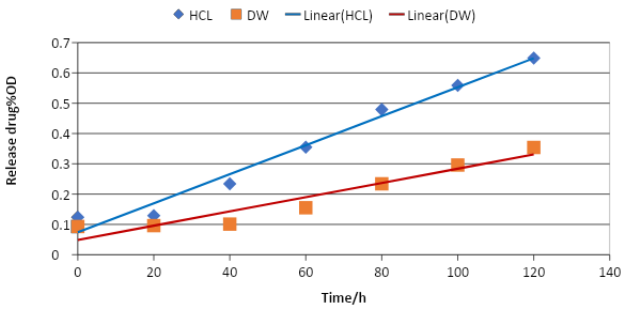

Figure 8. In vitro drug release assay(IVRT) of $CoFe_2O_4$ ($CoFe_2O_4$ NPS stock in dialysis bag soaked in distilled water, and $CoFe_2O_4$ NPS stock in dialysis bag soaked in Hcl solution).

dilatations. While spleen section of $CoFe_2O_4$ nanoparticles treated animals shows normal splenic architecture with very mild vascular congestion. As shown in figure (9: G2).

Microscopical examination of the liver in group injected with $CoFe_2O_4$ nanoparticles(G3) LD50% dose (3000 mg/kg b.w i.p.) as one dose .Shows marked central vein dilatation and congestion with red blood cells surrounded by multifocal hepatocytes cytoplasmic hydropic degeneration and nuclear enlargement with well-defined sinusoidal dilatation and congestion. Histopathological section of mice heart shows extensive multifocal vascular dilatation and congestion, mild perivascular inflammatory cells infiltration, and no ischemic necrosis of cardiomyocytes. While kidney shows marked vascular dilatation and congestion, interstitial and glomerular vascular space with multifocal tubular degeneration and inflammatory cells in the interstitial tissue. Microscopical examination of mice spleen shows red pulp and white pulp expansion with extensive multifocal hemorrhagic areas with vascular dilatation and congestion. As shown in figure (9: G3).

The results demonstrated that $CoFe_2O_4$ nanoparticles at a dose of 75 mg/kg body weight intraperitoneally showed no significant differences when compared with the normal control group. While there's a substantial difference between the group that was injected with LD50 percent. (Eman *et al.,*2021).

Histopathological alterations found in the group that was given injections of $CoFe_2O_4$(75mg/kg) NPs showed a structure of the hepatic architecture that was similar to that of a normal mouse, despite the presence of subtle modifications in the hepatic tissue, such as congested blood vessels and enlargement of blood sinusoids. In addition, it was discovered that mice who had been treated with CF NPs had normal renal tubules, normal renal cortex, and normal glomeruli with regular Bowman's capsule. (Abdel-Aziz *et al.,* 2018).

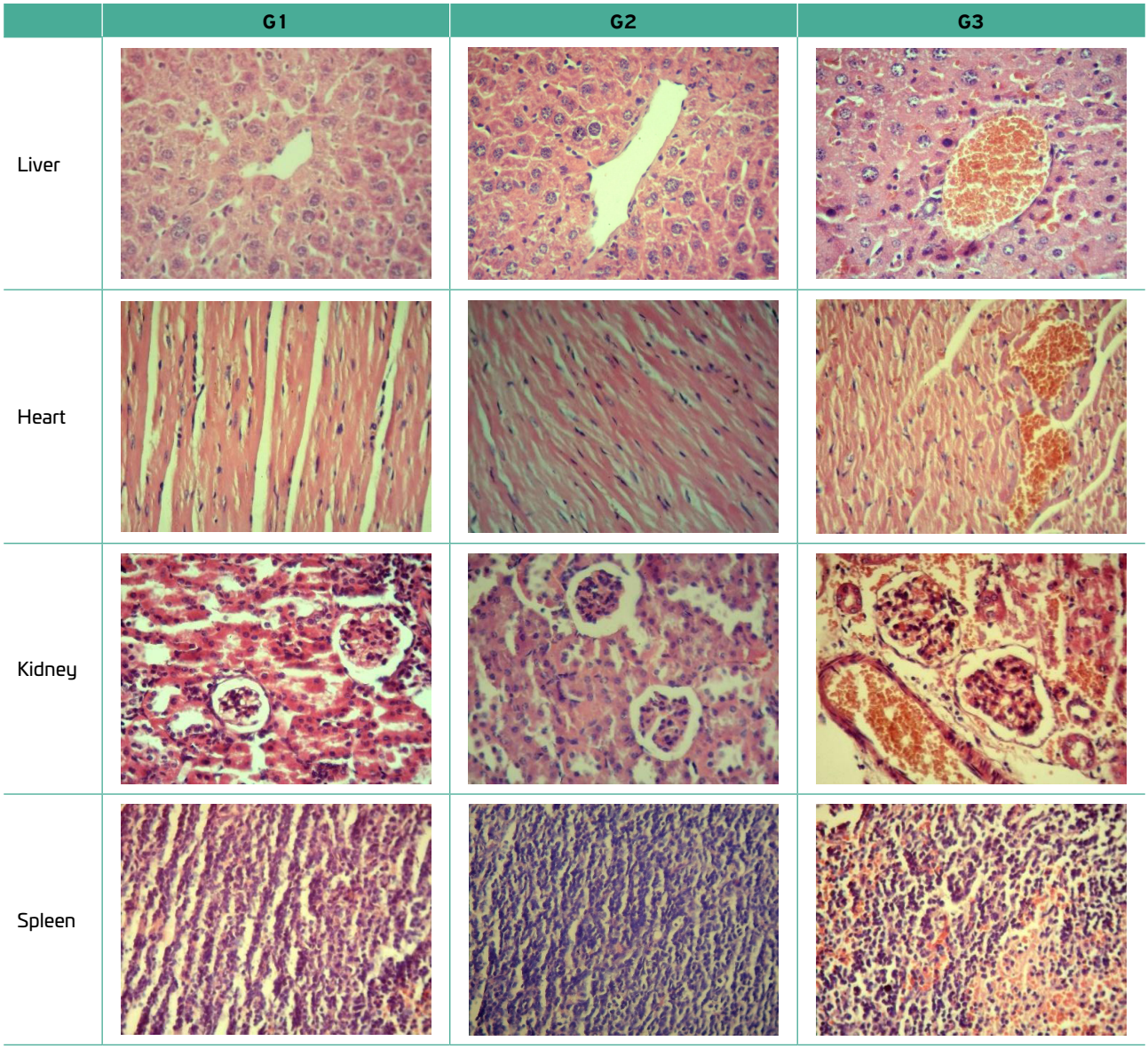

Figure 9. Histopathological changes of different mice tissues after 14 days in G1(negative control group) injected with saline (10ml/kg b.w)i.p, G2injected with $CoFe_2O_4$ (75mg/kg b.w)i.p, and G3 injected with $CoFe_2O_4$ (3000mg/kg b.w)i.p, (H&E stain 40X).

As can be seen, there was no mortality between the $CoFe_2O_4$ nanoparticles-treated animals and the control mice when administered at doses ranging from 2250 to 2750 g / kg/ bw. In addition, neither the control group nor the treatment group displayed any clinical symptoms or behaviors that were out of the ordinary, (Tanta *et al.,* 2021) mention the absence of vocalizations, labored breathing, difficulties in moving, hunching, also, there were no redness, swelling, or unusual activities. The obtained results indicate that $CoFe_2O_4$ nanoparticles are not toxic at concentration 1/40 of 3g/kg b.w.

There are not many publications available on the toxicity of Fe_3O_4. For instance, some research has revealed non-toxic effects under in vivo settings, while others have described minimal toxicity (Kim *et al.,* 2006). In vivo studies have shown that some subjects experienced liver and kidney damage, as well as abnormalities in their gastrointestinal and neurological systems. (Arora *et al.,* 2012; Amiri and Shokrollahi, 2013). Cobalt-induced cardiomyopathy was observed due to mitochondrial changes are representative of disturbance in energy production/utilization. (Packer.,2016). The expansion and plethora of blood vessels, determined in some organs, may be a manifestation of reactive changes caused by certain concentrations of $CoFe_2O_4$nanoparticles. (Anastasiia *et al.,*2021).

As seen in previous results Cobalt ferrites elicit dose-dependent genotoxicity and cytotoxicity in a variety of organisms, including mouse models (Abudayyak *et al.,* 2017), human, guinea pig, and algae. (Kapilevich *et al.,* 2010). And this cytotoxicity due to the ability of Cobalt NPs are capable of causing the creation of ROS, which can damage cellular DNA (Li *et al.,* 2020).

CONCLUSION

In summary, the pulse laser deposition technique was able to produce CoFe2O4 as confirmed by detailed structural characterization. Analysis by XRD verified the crystalline nature and phase purity of CoFe2O4 nanoparticles, with an average size of 12nm estimated using Scherrer's formula.

FTIR results indicated the characteristic vibration modes of spinel cobalt ferrite. EDX spectroscopy further verified the presence of Co, Fe, and O in appropriate stoichiometric ratios. SEM images revealed the nano size and surface morphology with some agglomerations due to magnetic nature of nanoparticles.

The drug release assay showed that CoFe2O4 nanoparticles demonstrate better release profiles under acidic pH, indicating their potential efficacy for tumoricidal action. The in vivo toxicity evaluation in mice model revealed no observable histopathological alterations at low doses of 75 mg/kg body weight administered for 14 days. However, higher doses of 3000 mg/kg body weight showed pathological changes in vital organs like liver, kidney, heart and spleen - thereby indicating dose-dependent toxicity.

Overall, the study confirms the successful synthesis of cobalt ferrite nanoparticles using PLD method and a relatively low toxicity profile at lower doses through systematic in vitro and in vivo experiments. The findings suggest potential biomedical applicability of CoFe2O4 nanoparticles, however dose-optimization is necessary to mitigate toxicity concerns before practical usage. Further explorations in disease models can shed more light on their therapeutic index and efficacy.

REFERENCES

ABDEL-AZIZ, O.H. Ragab, E.E. and Hamdan, M.H. The histological effects of zinc oxide nanoparticles on the kidney of adult male rabbits. **J.of Sohag Medical**, 22 (2): 297-301, 2018.

AMIRI, S.; Shokrollahi H. . The role of cobalt ferrite magnetic nanoparticles in medical science. **Materials Science and Engineering**. C, 33(1), 1-8, 2013.

ANASTASIIA, S. Garanina, Alexey A. Nikitin, Tatiana O. Abakumova,Alevtina S. Semkina,Alexandra O. Prelovskaya,Victor A. Naumenko,Alexander S. Erofeev,Peter V. Gorelkin,Alexander G. Majouga,Maxim A. Abakumov, and Ulf Wiedwald. Cobalt Ferrite Nanoparticles for Tumor Therapy: Effective Heating versus Possible Toxicity. **Journals Nanomaterials** ,Volume 12 ,Issue 1 ,2022.

AN-HUI LU, An-Hui; E. L. Salabas; Ferdi Schüth. "Magnetic Nanoparticles: Synthesis, Protection, Functionalization, and Application". **Angew. Chem. Int.** Ed. 46 (8): 1222–1244, 2007.

ARORA, S; Sharma, P; Kumar, S. (2012) Gold-nanoparticle induced enhancement in growth and seed yield of Brassica juncea. **Plant Growth Regul.** 66: 303–310. https:/doi.org/10.1007/s10725-011-9649-z

BANCROFT JD, Gamble M. Theory and Practice of Histological Techniques. Churchill Livingstone/**Elsevier**, Philadelphia, PA, USA, pp. 725, 6th ed. 2008.

CHAITALI, D.,Arup G.,Manisha, A.,Ajay G.and Madhuri M.G. Improvement of Anticancer Drug Release by Cobalt Ferrite Magnetic Nanoparticles through Combined pH and Temperature Responsive Technique. **ChemPhysChem**,19(21): 2872_2878, 2018.

DIXON, W. J. "Efficient analysis of experimental observations." **Annual review of pharmacology and toxicology**, vol. 20, p. 441-462, 1998.

EMAN, T.; EL-Nahass,S.; A.EL-Naggar, B., Salem and Mona, M. **E. evaluation of toxic effect of cobalt/zinc/ferrite nano -complex in experimental mice**, 2021. doi.org/10.21203/rs.3.rs-941124/v1.

GHAZALEH, A.; Siti, M. T.; Payam, A. Magnetic properties of cobalt ferrite synthesized by hydrothermal method. **Int Nano Lett**. v. 5, p. 183–186, 2015. DOI 10.1007/s40089-015-0153-8.

HOSSEINI, S. M; Sohrabnejad, S. Nabiyouni, G. Jashni, Van der Bruggen, E. B.A. Magnetic cation exchange membrane incorporated

with cobalt ferrite nanoparticles for chromium ions removal via electrodialysis. **Journal of Membrane Science.** v. 583, p. 292-300, 2019.

KALAM, A., Al-Sehemi, A.G., Assiri, M., Du, G., Ahmad, T., Ahmad, I. and Pannipara, M. Modified solvothermal synthesis of cobalt ferrite (CoFe2O4) magnetic nanoparticles photocatalysts for degradation of methylene blue with H2O2/visible light. **Results in Physics**, v. 8, p. 1046-1053, 2018.

KAPILEVICH, L. *et al*. Effect of nanodisperse ferrite cobalt (CoFe2O4) particles on contractile reactions in guinea pigs' airways. **Bull Exp Biol Med**, nº 149, p.70, 2010.

KIM D-H, Lee S-H, Kim K.-N., Kim K-M, Shim I-B, Lee Y-K. Cytotoxicity offerrite particles by MTT and agar diffusion methods for hyperthermic application. **J Magn Magn Mater**. 293:287–92, 2005.

KIM, D., Jeong, S. and Moon, J. Synthesis of silver nanoparticles using the polyol process and the influence of precursor injection. **Nanotechnology**, v. 17, p. 4019–4024, 2006.

KIM, DK, G.; Mikhaylova, M; *et al*. "Anchoring of Phosphonate and Phosphinate Coupling Molecules on Titania Particles". **Chemistry of Materials**. nº 15, v. 8, p. 1617–1627, 2003.

LI S, Li H, Xu X, Saw PE, Zhang L. Nanocarrier-mediated antioxidant delivery for liver diseases. **Theranostics**. nº 10, v. 3, p. 1262-1280, 2020. doi:10.7150/thno.38834.

LU A.-H.; Salabas E. L.; Schüth F. "Magnetic Nanoparticles: Synthesis, Protection, Functionalization, and Application". **Angew. Chem. Int.** Ed. 46, v. 8, p. 1222–1244, 2007.

M.W. Mushtaq1 , M. Imran1 , S. Bashir2 , F. Kanwal1 , L. Mitu3(2016). Synthesis, structural and biological studies of cobalt ferrite nanoparticles. B**ulgarian Chemical Communications**, Volume 48, Number3, p. 577– 582, 2016.

MAAZ, K., Mumtaz, A., Hasanain, S. K., & Ceylan, A. Synthesis and magnetic properties of cobalt ferrite (CoFe2O4) nanoparticles prepared by wet chemical route. **Journal of magnetism and magnetic materials**, v. 2, p. 289-295, 2007.

MAHMOUD, A.; Tuba, A. G.; Gül, Ö. In Vitro Toxicological Assessment of Cobalt Ferrite Nanoparticles in Several Mammalian Cell **Types Biological Trace Element Research**, volume 175, p. 458–465, 2007.

MAHMOUD, G. N.; Elias, B. S.; Hossein, A. A.; Abdul, H. S.; Mansor, H. **Simple Synthesis and Characterization of Cobalt Ferrite Nanoparticles by a Thermal Treatment Method**. 2010 |Article ID 907686 | https://doi.org/10.1155/2010/907686

MOHAMMAD, H., Shahsavari, A., Adel, M., Iman, R. and Shadie H. Distribution of "molybdenum disulfide/cobalt ferrite" nanocomposite in animal model of breast cancer, following injection via differential infusion flow rates. **Journal of Pharmaceutical Investigation**, v. 50, p. 583–592, 2020.

MORA, L., Chumbimuni-Torres, K. Y., Clawson, C., Hernandez, L., Zhang, L., Wang, J. (2009). Real-time electrochemical monitoring of drug release from therapeutic nanoparticles. **Journal of Controlled Release**, v. 1, p. 69-73.

MUKTA, V. Limaye, Shashi B. Singh, Sadgopal K. Date,Deepti Kothari, V. Raghavendra Reddy, Ajay Gupta,Vasant Sathe, Ram Jane Choudhary, and Sulabha K. Kulkarni. "High coercivity of oleic acid CoFe2O4 nanoparticles at room temperature". **J. Phys. Chem**. B 113, p. 9070-9076, 2009.

NLEBEDIMN, I. C., Ranvah, N., Williams, P. I., Melikhov, Y., Snyder, J. E., Moses, A. J; Jiles, D. C. Effect of heat treatment on the magnetic and magnetoelastic properties of cobalt ferrite. **J. of Magn. Magn. Mater.** p. 1929–1933, 2010.

PACAKOVA, B; Kubickova, S; Reznickova, A; Vejpravova, D. N, J. Spinel ferrite nanoparticles: correlation of structure and magnetism. In: Magnetic Spinels – Synthesis, Properties and Applications. M Seehra (Ed.). IntechOpen Limited, London, UK 2017.

PRASHANT, B. Kharat, J. S. Kounsalye, M. V. Shisode, K. M. **Preparation and Thermophysical Investigations of CoFe2O4-based Nanofluid: a Potential Heat Transfer Agent Journal of Superconductivity and Novel Magnetism.** 2018 https://doi.org/10.1007/s10948-018-4711-y.

RAUT, A. V., Barkule, R. S., Shengule, D. R., & Jadhav, K. M. Synthesis, structural investigation and magnetic properties of Zn2+ substituted cobalt ferrite nanoparticles prepared by the sol–gel auto-combustion technique. **Journal of Magnetism and Magnetic Materials**, 358, 87-92, 2014.

SALAS, G., Costo, R., & Morales, M. D. P. **Synthesis of inorganic nanoparticles**. Frontiers in Nanoscience, v. 4, p. 35-79, 2012.

SOOD, M.. A. and Khudiar, K. K. Role of Salvia officinal,s silver Nano-particlesin Attenuating Renal Damage in Rats Exposed to Methotrexate (part 1). **The Iraqi Journal of Veterinary Medicine**. v. 2, p. 7-20, 2019.

SUMAIAH, I. Hussein, S. S. Shubber, Nahi, Y. Bio-distribution of Gold Nanoparticles in Tumor Mass and Different Organs in Implanted Mice with Mammary Adenocarcinoma AM3 (in vivo study) .**The Iraqi Journal of Veterinary Medicine.** v. 2, p. 17-22, 2019.

TANTA, E. EL-Nahass, Sabry, A. EL-Naggar,Basant; Salem, I. Mona, M. **Evaluation of toxic effect of cobalt/zinc/ferrite nano -complex in experimental mice**, 2021. DOL:http/doi.org/10.21203/rs.3.rs-941124/v1.